The Canadian Mineralogist
Vol. 40, pp. 1609-1627 (2002)

OCCURRENCE OF LOW-Ti AND HIGH-Ti FREUDENBERGITE IN ALKALI SYENITE DIKES FROM THE KATZENBUCKEL VOLCANO, SOUTHWESTERN GERMANY

VOLKER STÄHLE[§] AND MARIO KOCH

Mineralogisches Institut, University of Heidelberg, Im Neuenheimer Feld 236, D-69120 Heidelberg, Germany

CATHERINE A. MCCAMMON

Bayerisches Geoinstitut, University of Bayreuth, D-95440 Bayreuth, Germany

UTE MANN AND GREGOR MARKL

Institut für Mineralogie, Geowissenschaften, University of Tübingen, Wilhelmstr. 56, D-72074 Tübingen, Germany

ABSTRACT

Freudenbergite ($Na_2Fe^{3+}{}_2Ti_6O_{16}$) occurs in peralkaline alkali syenite dikes at Katzenbuckel, southwestern Germany, in association with lorenzenite, pyrochlore, landauite and Na–Zr silicates as rare, late-stage mineral phases. Freudenbergite shows a broad range in chemical composition; we recognize two varieties: 1) a "low-titanium" type, with low concentrations of Ti and all iron in the trivalent state, as established by Mössbauer spectroscopy; this is the normal type of freudenbergite found in a syenite from the Katzenbuckel; 2) a "high-titanium" type, with elevated concentrations of Ti and high contents of divalent cations (Mg^{2+}, Mn^{2+}, Zn^{2+}) substituting for Fe^{2+}. Increased concentrations of Nb are the cause of cation deficiency of sodium at the *A* site. Freudenbergite, up to 0.75 mm in size, is a sector-zoned mineral with selective enrichments in (Nb + Zr) and Ti in sectors (001) and (100), respectively. In one dike (Kb 45), freudenbergite metasomatically replaces primary ilmenite as well as thin exsolution-lamellae within hematite grains. Pseudobrookite, ilmenite, hematite or magnetite occur as Fe–Ti oxides in the freudenbergite-bearing syenite samples. Ilmenite–hematite mineral pairs show large miscibility-gaps, and indicate conditions of formation in the range of 750–550°C at low pressures of about of 0.2–0.3 kbar. The unique occurrence of primary freudenbergite is mainly due to an efficient process of fractionation of the peralkaline syenitic melt, leading to a Na- and Ti-rich, but Ca-poor melt accompanied by a distinct enrichment in niobium and zirconium.

Keywords: freudenbergite, chemical composition, sodium–iron–titanium oxide, volcanic rocks, alkali syenite, Katzenbuckel, Germany.

SOMMAIRE

La freudenbergite ($Na_2Fe^{3+}{}_2Ti_6O_{16}$) est présente dans des filons de syénite hyperalcaline à Katzenbuckel, dans le sud-ouest de l'Allemagne, en association avec lorenzenite, pyrochlore, landauite et des silicates de Na–Zr comme manifestations tardives de cristallisation. Elle montre un intervalle de composition important; nous en documentons deux variétés: 1) une variété à teneur en Ti relativement faible, avec tout le fer sous forme trivalente, ce qui a été confirmé par spectroscopie de Mössbauer; il s'agit de la freudenbergite normale rencontrée dans la syénite de Katzenbuckel; 2) une variété à concentrations élevées de Ti et de cations bivalents (Mg^{2+}, Mn^{2+}, Zn^{2+}) à la place de Fe^{2+}. Des niveaux accrus de Nb sont la cause d'un déficit de sodium dans le site *A*. La freudenbergite, en cristaux atteignant 0.75 mm, montre une zonation en secteurs, avec un enrichissement sélectif en (Nb + Zr) et Ti dans les secteurs (001) et (100), respectivement. Dans un filon (Kb 45), la freudenbergite remplace par métasomatose l'ilménite primaire, de même que de minces lamelles d'exsolution au sein de cristaux d'hématite. La pseudobrookite, l'ilménite, l'hématite ou la magnétite sont les oxydes de Fe–Ti présents dans les échantillons de syénite porteurs de freudenbergite. Les paires ilménite–hématite font preuve de larges lacunes de miscibilité, et indiquent une cristallisation sur l'intervalle 750–550°C à faible pression, environ 0.2–0.3 kbar. Le développement unique de la freudenbergite primaire serait surtout dû à un processus efficace de fractionnement d'un liquide syénitique à néphéline, ce qui a mené à un liquide évolué riche en Na et Ti, mais dépourvu de Ca, et anormalement enrichi en niobium et en zirconium.

(Traduit par la Rédaction)

Mots-clés: freudenbergite, composition chimique, oxyde de sodium–fer–titane, roches volcaniques, syénite hyperalcaline, Katzenbuckel, Allemagne.

§ *E-mail address*: vstaehle@min.uni-heidelberg.de

Introduction

The volcanic Katzenbuckel alkaline complex, the type locality of freudenbergite, ideally $Na_2Fe^{3+}{}_2Ti_6O_{16}$ (Frenzel 1961), is located in southern Germany, within the southeastern part of the Odenwald, about 25 km east of Heidelberg (Fig. 1). At this location, a basaltic protrusion (of about 100 m) overlooks the Pliocene peneplane of the Winterfeld, cutting sedimentary Upper Buntsandstein (so_1) strata. The wooded hilltop is the surficial remnant of a deeply eroded eruption cylinder, about 1 km in diameter.

The lack of a systematic study on freudenbergite from the Katzenbuckel volcanic neck motivated this investigation. Our objectives are, firstly, to check in which type of rocks the mineral freudenbergite occurs; so far, it has been found only within a single boulder of syenite (Frenzel 1961). Secondly, we wish to ascertain the compositional range of freudenbergite, especially with regard to the predicted coupled substitution $2\ Fe^{3+} \rightleftharpoons Fe^{2+} + Ti^{4+}$. Published chemical data are sparse; Patchen *et al.* (1997) have divided their samples of kimberlitic affinity into ferrous and ferric freudenbergite. Thirdly, we consider the reason the Katzenbuckel volcanic rocks contain freudenbergite as a primary magmatic phase, whereas comparable alkaline rocks elsewhere apparently do not.

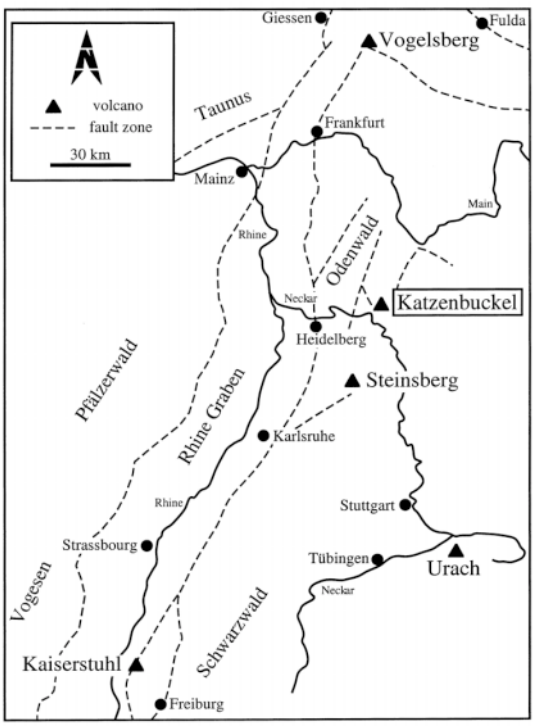

FIG. 1. Sketch map from the Rhine graben area (eastern France and southwestern Germany) with location of the Katzenbuckel complex ~30 km east of Heidelberg. Modified after Calvez & Lippolt (1980).

Background Information

The 66 Ma old Katzenbuckel rocks (Lippolt *et al.* 1963, 1976) and numerous exposures of volcanic rocks in the Upper Rhine graben area belong to the larger Central European Volcanic Province (Wimmenauer 1974, Wilson & Downes 1991). These rift-related extrusions bear witness of a long period of volcanic activity lasting from the early Mid-Cretaceous to the Late Tertiary.

A peculiarity of the Katzenbuckel sanidine nephelinites and sodic shonkinites is their unusually high alkalinity and low SiO_2 concentrations. In an alkali silica diagram (TAS), these rocks plot far offside parental olivine nephelinites or other volcanic rocks that are found in this magmatic province (Gehnes & Wimmenauer 1975).

Katzenbuckel is a world-famous locality. The first period of scientific research, more than 175 years long, has put forth numerous contributions, among others from von Leonhard & Gmelin (1822), Rosenbusch (1869) and Freudenberg (1906). Recently, a petrographic summary of the Katzenbuckel rocks was given by Frenzel (1975).

Freudenbergite may be expressed by the general formula $A_xB_yT_{8-y}O_{16}$ (Haggerty 1983). In the formula, *A* represents the larger cations Na^+, K^+, Rb^+, whereas the smaller ones like Al^{3+}, Cr^{3+}, Fe^{3+}, Fe^{2+}, Mg^{2+}, Mn^{2+}, Zn^{2+}, Ni^{2+}, Co^{2+}, Cu^{2+} are positioned at *B*, and equally sized, more highly charged ions like Ti^{4+}, Zr^{4+}, Nb^{5+} are placed at *T*. Based on the coupled substitution $2\ R^{3+} \rightleftharpoons R^{2+} + R^{4+}$, freudenbergite forms an extensive solid-solution series between the end-members $Na_2Fe^{2+}Ti_7O_{16}$ and $Na_2Fe^{3+}{}_2Ti_6O_{16}$.

Niobium-rich and niobium-poor varieties have been found with the electron microprobe (Frenzel *et al.* 1971), being almost identical in composition to two samples of freudenbergite analyzed by McKie & Long (1970). The proportion of iron in these samples, calculated as Fe^{3+}, is in good accordance with an experimental study of Flower (1974), according to which freudenbergite is stable at high oxygen fugacities, near the Mn_2O_3–Mn_3O_4 buffer, and high H_2O pressures (1000 bars) over a temperature range of 700–900°C.

Freudenbergite is monoclinic (*C*2/*m*) with unit-cell dimensions of *a* 12.305, *b* 3.822, *c* 6.500 Å and with $\beta = 107.30°$ (McKie 1963, McKie & Long 1970). Its crystal structure is similar to that of synthetic sodium–titanium dioxide "bronze", $Na_{0.22}(Ti,Fe)O_2$ (Wadsley 1964, Bayer & Hoffmann 1965, 1966).

Structural refinements of $Na_{2.00}Fe_{2.00}Ti_{6.00}O_{16}$ yielded edge- and corner-sharing $(Ti,Fe)O_6$ octahedra, with double sheets parallel to (001), forming an open

framework structure where larger Na^+ ions fit into the open spaces, stabilizing the structure (Ishiguro *et al.* 1978, Prestel 1992, Wadsley 1964). Furthermore, the $(Fe,Ti)O_6$ octahedra split into $M(1)$ and $M(2)$ sites, over which Ti^{4+} and Fe^{3+} are randomly distributed.

Ferrous-iron-dominant freudenbergite ($Na_2Fe^{2+}Ti_7O_{16}$) has been reported from lower-crust granulites (Liberia), upper-mantle xenoliths (South Africa) and ilmenite megacrysts (Yakutia) entrained in kimberlites (Haggerty 1983, 1987, Patchen *et al.* 1997). Whereas these samples of Fe^{2+}-bearing freudenbergite are interpreted to be of metasomatic origin, the Katzenbuckel samples so far represent the only examples of "orthomagmatic" freudenbergite worldwide.

Geological Setting of the Katzenbuckel Volcano and Occurrence of the Freudenbergite-Bearing Samples

At the time of eruption, in the Upper Cretaceous, the eastern Odenwald was covered by a 600-m-thick pile of Muschelkalk, Keuper and Jurassic sedimentary rocks (Frenzel 1975). The present erosional surface cuts through a subvolcanic level of the Katzenbuckel complex. Large fragments of Jurassic rocks, brecciated *in situ*, are embedded within a tuffaceous fallback breccia (Schlotbreccia). The sedimentary boulders are strongly indicative of an explosive mechanism of eruption.

The volcanic formation can be studied in old and abandoned quarries, Gaffstein and Michelsberg, where various types of alkaline rocks occur (Frenzel 1975, Okrusch *et al.* 2000). More than 90% of the volcanic suite consist of "basaltic", fine-grained sanidine nephelinites, whereas on the eastern side of the volcanic neck, a small, stock-like body of coarse-grained shonkinite has been emplaced. The two rock types are quite similar in chemical and mineralogical composition (Frenzel 1967).

Nepheline–mica porphyries, alkali syenites and greenish tinguaites occur in late, evolved dikes cutting the sanidine nephelinite and shonkinite. The alkali syenites are very sodium-rich, whereas the greenish tinguaites show a characteristically high potassium content.

Centimeter-sized veins of apatite and magnetite, lenses of sulfide minerals, pseudobrookite and hematite pockets as well as tuffaceous material, locally converted to sanidine, make up the late products of pneumatolytic activity within the Katzenbuckel complex (Frenzel 1967, 1975).

Freudenbergite was originally found in a sample of yellow-brown alkali micro-syenite (Frenzel 1960, 1961) in the Katzenbuckel collection of the Mineralogical Institute of the University of Heidelberg. The sample was collected in 1926 as a large specimen at the summit of the Michelsberg, close to the southwestern corner of the Michelsberg quarry (Alter Gemeindesteinbruch; see Frenzel 1955, 1960).

We found that from a collection of 17 pieces of different alkali syenite dikes, only nine samples contain freudenbergite. Five of these freudenbergite-bearing specimens were taken from the institute's Katzenbuckel collection, among them the type-locality freudenbergite-bearing rock (Kb 41). The remaining freudenbergite-containing samples were collected recently at the abandoned Michelsberg quarry.

Analytical Procedures

Mineral analyses were performed using a CAMECA SX–51 electron microprobe (Mineralogical Institute, University Heidelberg) equipped with five wavelength-dispersion spectrometers. Operating conditions were: beam current 20 nA and accelerating voltage 15 kV, with a beam diameter of about 1 μm. Natural as well as synthetic silicate and oxide standards [wollastonite (Si, Ca), rutile (Ti), baddeleyite (Zr), niobium oxide (Nb), corundum (Al), chromium oxide (Cr), hematite (Fe), rhodonite (Mn), magnesium oxide (Mg), vanadium oxide (V), albite (Na) and orthoclase (K)] were used for calibration. The data were corrected using the PAP algorithm. Back-scattered electron (BSE) images and energy-dispersion element-distribution maps were obtained from a LEO 440 scanning electron microscope, equipped with an Oxford semiconductor detector using an accelerating voltage of 20 kV and a beam current in the nA range.

The samples were analyzed for major and trace elements by X-ray fluorescence (Siemens SRS 3000) using melted and pressed whole-rock powder tablets, prepared in an agate mortar (Laboratory of Terrachem, Mannheim, Germany).

Mössbauer spectra were recorded at room temperature (293 K) in a transmission mode with a constant-acceleration Mössbauer spectrometer with a nominal 370 MBq ^{57}Co high-specific-activity source (148 GBq/cm^2) in a 12 μm Rh matrix (see McCammon *et al.* 1991, McCammon 1994). The velocity scale was calibrated relative to a 25 μm α-Fe foil using the positions certified for the National Bureau of Standards standard reference material no. 1541; line widths of 0.34 mm/s for the outer lines of α-Fe were obtained at room temperature. Five crystals, each approximately 200 μm in diameter, were placed within a hole of 500 μm that was drilled into a *ca.* 100 μm thick Pb foil. The crystals were held in place with cellophane tape. The effective thickness of the absorber is approximately 5 mg Fe/cm^2 based on the chemical composition and sample geometry. The spectrum was collected over three days. The spectra were fitted using the commercially available fitting program NORMOS written by R.A. Brand (distributed by Wissenschaftliche Elektronik GmbH, Germany).

Mineralogy and Petrography of the Freudenbergite-Bearing Dike Rocks

Both the nephelinite and sodic shonkinite contain thin veins of syenite 1–5 cm in width. One horizontally intruded dike or sill at the Michelsberg quarry shows a larger thickness, in the range of 15–40 cm. The sodic shonkinite stock contains more dikes, possibly because it offered better pathways for the magma (Frenzel 1955).

Modal variations of sanidine and sodic pyroxenes allow us to distinguish two types of alkali syenite: a leucocratic one, light yellow to reddish, is characterized by the preponderance of sanidine, whereas a mesocratic, greenish variety is richer in aegirine or aegirine–augite. Since aegirine is the more common sodic pyroxene in these samples, we will refer to the clinopyroxene as aegirine. As the modal proportion of nepheline and analcime increases, the syenite merges into tinguaite.

Medium- to coarse-grained syenite dikes show a "pegmatite"-like appearance and, in many cases, are symmetrically zoned. Tabular feldspars and, to a lesser extent, pyroxene and amphibole, grow at approximately right angles to the contact of the dikes. This arrangement of mineral growth results in a comb-like fabric (Fig. 2). The central part of the dikes is occupied by non-oriented, finer-grained aggregates of minerals or a dense, opaque matrix.

The main constituents in the dikes are sanidine (Or_{52}–Or_{90}), zirconium-bearing aegirine with regular or patchy zonations, and a Ti-rich katophoritic to arfvedsonitic amphibole. The aegirine is prismatic or fibrous, whereas the grains of amphibole are tabular or lamellar. In general, the sanidine laths show Carlsbad-twinning. Some alkali syenite samples contain small flakes of a Ti-rich biotite. Crystals of nepheline commonly show a hexagonal cross-section up to 0.5 cm across, but are usually replaced by natrolite (Fig. 2). In one case, small, jagged remnants of pre-existing nepheline were found within a partly replaced grain. Tiny needles of apatite are only present in the matrix of syenite Kb 34 as a late magmatic phase.

Most alkali syenite dikes contain larger, euhedral laths of sanidine crystals with open spaces of variable size. It is in such cavities that fine-grained natrolite or accessory phases like freudenbergite, Fe–Ti oxides, pyrochlore, landauite and rare Na–Zr minerals are predominantly found (Fig. 2).

Coexisting with freudenbergite, the alkali syenites may contain accessory Fe–Ti oxide phases like pseudobrookite, ilmenite, hematite or magnetite in highly variable proportions (Table 1).

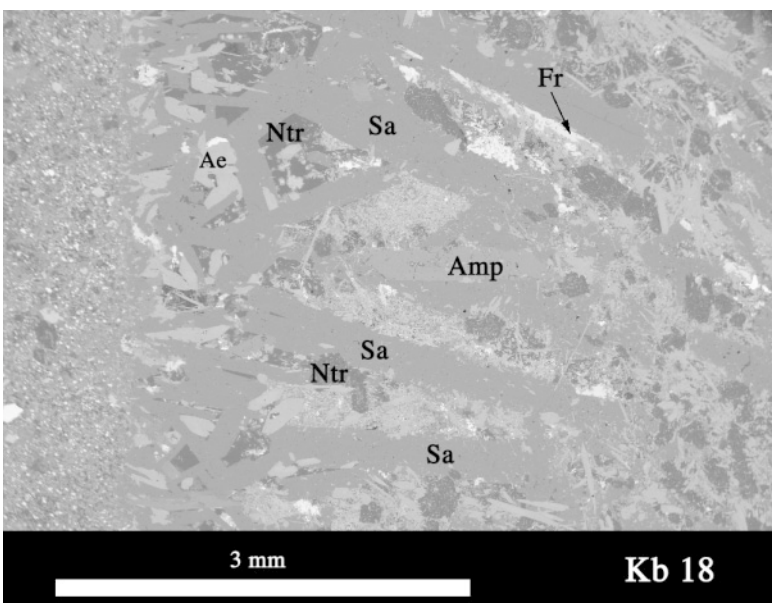

FIG. 2. BSE image from a small segment of alkali syenite dike Kb 18. Sanidine laths (Sa) are arranged approximately perpendicular to the intrusion rims. In the interspaces, freudenbergite crystals (Fr; white) and rare, late-stage mineral phases (Na–Zr silicates; white) occur predominantly. Dark hexagonal patches are natrolite (Ntr) pseudomorphs after nepheline. Grains of amphibole (Amp) and aegirine (Ae) are the coexisting mafic minerals.

Textural Attributes and Chemical Composition of Freudenbergite

Textural attributes

Freudenbergite is an accessory phase in most of the alkali syenite samples. In the discovery sample, freudenbergite is mostly angular and anhedral, but occasionally the grains show an excellent tabular shape with a length of 0.15 mm and a width of 0.05 mm on average (Frenzel 1961). However, within some leucocratic, sanidine-rich samples, it forms a minor constituent of up to 5 vol.%. In most cases, the mineral is euhedral or subhedral, showing a prismatic or tabular shape up to 0.75 mm across (Fig. 3). The majority of freudenbergite crystals are tabular parallel to (010) or elongate parallel to [100] or [001].

In transmitted light, freudenbergite is slightly translucent. The mineral is pleochroic and shows dark brown to slightly yellow brown absorption-colors and occasionally also simple twins. However, in thicker sections, freudenbergite is totally opaque. A faint bireflectivity is seen in reflected light, and yellow-brown internal reflections are quite common.

TABLE 1. LIST OF THE FREUDENBERGITE-BEARING ALKALI SYENITE DIKES WITH COEXISTING Fe–Ti OXIDES, KATZENBUCKEL VOLCANO, SOUTHWESTERN GERMANY

	Pseudobrookite	Ilmenite	Hematite	Magnetite
Kb 18	–	×	×	–
Kb 34	–	–	–	–
Kb 40	–	–	–	–
Kb 41	–	–	×	×
Kb 42	–	×	×	×
Kb 45	–	×	×	×
Kb 50	×	×	×	×
Kb 51	–	×	×	×
Kb 59	×	×	×	–

The symbol × denotes that the phase is present, and –, that it is absent.

Sector-zoning and chemical composition of freudenbergite

Many grains of freudenbergite show symmetrical sector-zoning. Usually invisible in the polarizing microscope, the chemical zoning was detected using BSE images.

Peralkaline nepheline syenite liquids present favorable conditions for the formation of sector-zoning (Larsen 1981); such zoning in minerals expresses the chemical selectivity on different crystal faces as a result of rapid growth (Jensen 2000).

A section of a sector-zoned, euhedral crystal of freudenbergite parallel to (010) is shown in Figure 4. The section is nearly perpendicular to the *b* direction, which is recognizable owing to the existence of the β

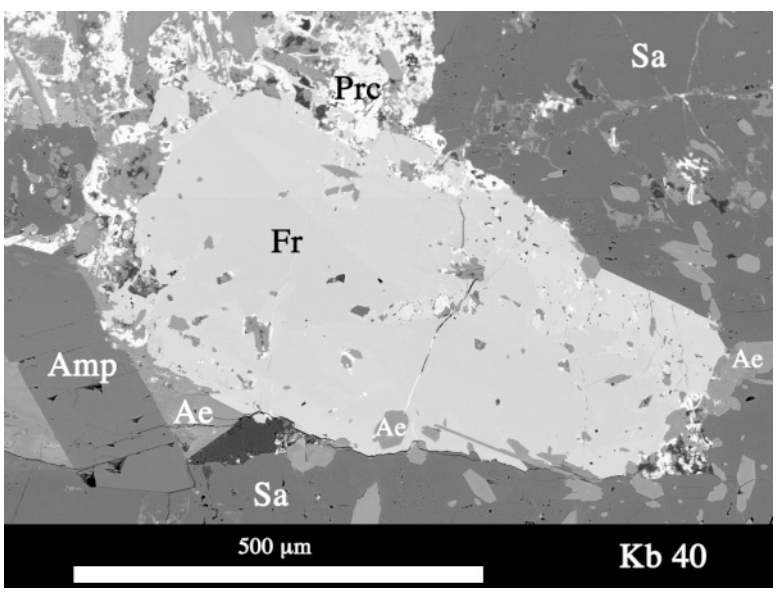

FIG. 3. BSE image of a large crystal of freudenbergite. Note the intergrowth of smaller grains of aegirine (Ae). Amphibole (Amp), aegirine (Ae), sanidine (Sa) and pyrochlore (Prc) are found surrounding freudenbergite.

angle of ~107°, at the upper left corner of the crystal. Growth sectors are essentially pyramidal in form, with a given face at the base and the top pointing to the interior of the crystal (Dowty 1976). In Figure 4, the base of the brighter sector is (001), whereas (100) is representative of the darker sector.

Five electron-microprobe analyses were obtained from each sector along the profile A – B – C in the crystal shown (Fig. 4). In the brighter sector, along traverse B – C, niobium and zirconium are clearly enriched, whereas within the darker sector, along the line A – B, higher concentrations of titanium were detected (Fig. 5). Freudenbergite concentrates minor elements like niobium and zirconium in sector (001) and also likely in sector (010).

Numerous grains of freudenbergite from nine different alkali syenite dikes have been chemically analyzed with an electron microprobe. More than 200 analyses demonstrate the large range in chemical composition of the mineral (Fig. 6, Tables 2, 3). In the diagram, they plot in two separate areas. The majority plot in the lower right of the diagram, within a *T*-site occupancy between 6.0 and 6.3 (Fig. 6). Hence, most compositions lie close to the freudenbergite end-member $Na_2Fe^{3+}{}_2Ti_6O_{16}$. With relatively low contents of Ti + Nb + Zr on the *T* site, such grains of freudenbergite may be termed "low-titanium" freudenbergite. They represent the common type of freudenbergite found in Katzenbuckel rocks according to four compositions (Fig. 6) given by McKie & Long (1970) and Frenzel *et al.* (1971). Moreover, in the examples of the "low-titanium" freudenbergite, total iron is dominantly in the trivalent state, which is verified by Mössbauer spectroscopy (see below).

Together with the "low-titanium" normal type, a second type of freudenbergite was found in some of the alkali syenite dikes (samples Kb 34, Kb 40, Kb 59). It is characterized by higher contents of TiO_2 + Nb_2O_5 + ZrO_2, and low concentrations of total iron (Table 3). These compositions are comparable to those of freudenbergite found in kimberlitic rocks (Fig. 6; Patchen *et al.* 1997). However, owing to their small grain-size (<<100 μm; Fig. 7), Mössbauer spectroscopy measurements on "high-titanium" freudenbergite grains could not be performed.

"High-titanium" freudenbergite occurs in two subtypes. At the edge of some larger crystals of freudenbergite in samples Kb 34 and Kb 40, there are small areas of variable chemical composition. Darker colored than the main grain, these tiny areas (<100 μm across) are only visible in BSE images. Analyses yielded higher concentrations of Ti, up to 76 wt.% TiO_2 (Table 3, anal. Kb 34–10, Kb 40–60), much more than in the core of the same crystals, which have a lower Ti content, in the range of 67–70 wt.% TiO_2.

The other member of the "high-titanium" group is more conspicuous and was found in Kb 59 as single, euhedral crystals (Fig. 7). Besides their high contents of Ti at the *T* site, these grains of freudenbergite have rather

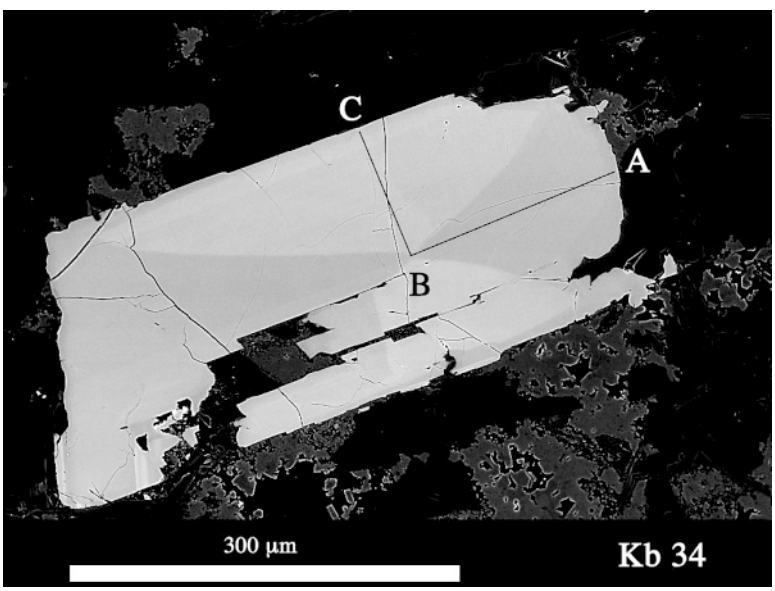

FIG. 4. BSE image of a sector-zoned crystal of freudenbergite. The chemical composition of the mineral was established along profile A–B–C with 10 analyses (Fig. 5). The bright pyramids correspond to sector (001), and the darker ones belong to sector (100).

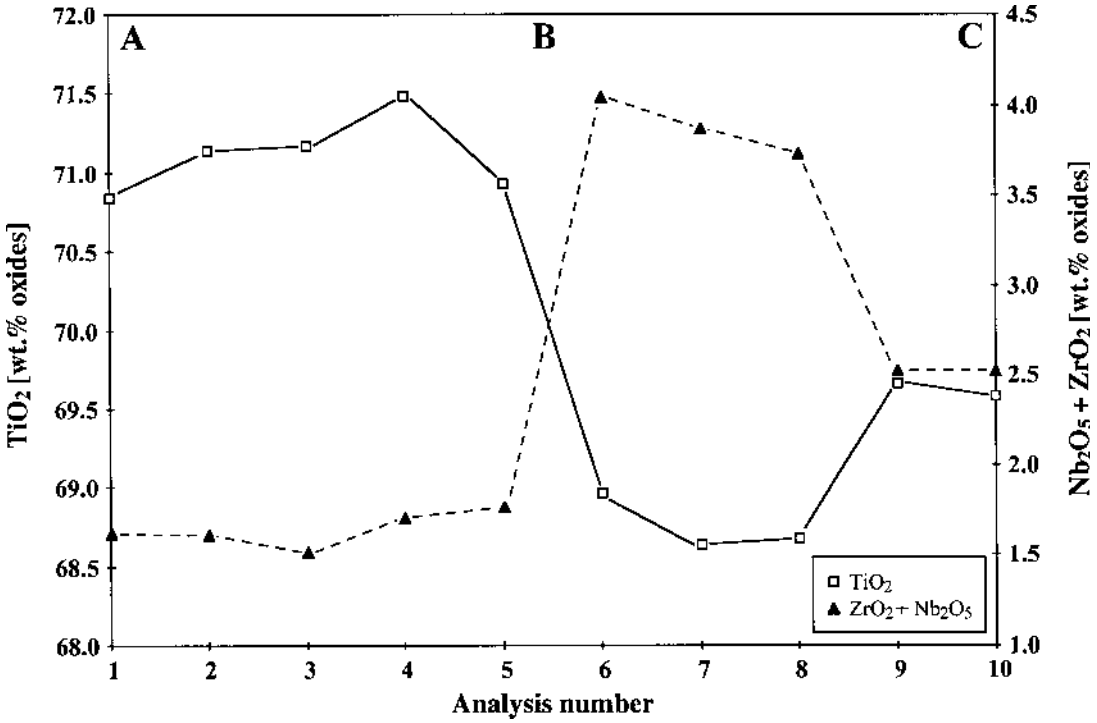

FIG. 5. Diagram with profile A–B–C of the sector zoned freudenbergite shown in Figure 4. In both sectors, the contents of TiO_2 and (Nb_2O_5 + ZrO_2) are inversely correlated.

high contents of divalent ions. The sum (MgO + MnO + ZnO), 3.95 wt.%, is much higher than the average of 1.05 wt.% of the coexisting "low-titanium" freudenbergite in sample Kb 59 (Table 3). The small tabular crystals commonly occur together with the rare mineral landauite (Fig. 7).

Moreover, these tabular crystals of freudenbergite show exceptionally high Nb contents, up to 12 wt.% Nb_2O_5 (Table 3). These high concentrations of Nb cause an excess of positive charges in the structural formula. As expected, these niobium-rich crystals of "high-titanium" freudenbergite show lower contents of Na, in the range of 6.70 to 7.06 wt.% Na_2O (Table 3), which is indicative of vacancies at the *A* site. In contrast, analyses of normal "low-titanium" freudenbergite invariably demonstrate Na contents greater than 8.10 wt.% Na_2O (Table 2). According to its structural formula, freudenbergite ($Na_2Fe^{3+}{}_2Ti_6O_{16}$) should contain 8.84 wt.% Na_2O.

Mössbauer spectra of freudenbergite

Alkali syenite sample Kb 34, with abundant and "large", almost inclusion-free crystals of freudenbergite, was selected for Mössbauer spectroscopy. The crystals selected belong to the common "low-titanium" type of freudenbergite.

Data were fitted to two Lorentzian doublets, which were sufficient to account for all spectral absorption (Fig. 8). The spectra were fitted on the basis of (1) minimization of the number of parameters, and (2) a physically realistic fit to the spectra. Conventional constraints of equal-component widths and areas of the doublets were applied.

The large degree of line overlap prevents an unambiguous deconvolution of the spectrum based on the Mössbauer data alone, but structural considerations help to reduce the number of possible models for a fit. The asymmetry of the main absorption peak requires at least two singlets or doublets to fit the spectrum (asymmetry may be ruled out owing to texture effects or relaxation). Since the only cation sites available for Fe^{3+} to occupy have octahedral symmetry (Ishiguro *et al.* 1978), a two-singlet fit model can be ruled out on the basis that the center shifts are unrealistic for octahedral coordination (*e.g.,* McCammon 2000). Similarly, a fit with two doublets with similar quadrupole splitting but different center-shifts can be ruled out, since the difference in

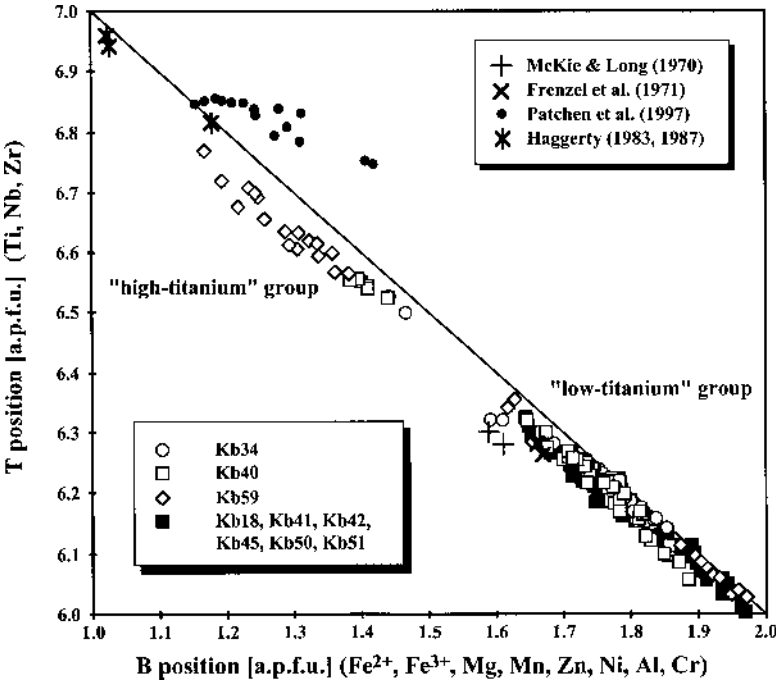

FIG. 6. Chemical composition of freudenbergite. Axes are plotted in atoms per formula unit. *T* represents (Ti + Nb + Zr) and *B* indicates the totals of (Fe^{3+} + Fe^{2+} + Mg + Mn + Zn). The compositions lie close to the line defining the substitution $2Fe^{3+} \rightleftharpoons Fe^{2+}$ + Ti. Owing to their different contents on the *T* and *B* sites, the compositions plotted are grouped into "low-titanium" and "high-titanium" variants. Filled symbols: "low-titanium" freudenbergite, the type present in various samples of syenite. Open symbols: representative compositions of the "high-titanium" and the "low-titanium" groups. In these samples, both types of freudenbergite occur. The published analytical data (Haggerty 1983, 1987, Patchen *et al.* 1997, McKie & Long 1970, Frenzel *et al.* 1971) are also shown in the diagram with different symbols (see box at upper right). If the compositions from Patchen *et al.* (1997) would be recalculated to have all iron in the trivalent state, they would plot in the same range as the "high-titanium" freudenbergite from this study.

center-shift values is too great to be consistent with octahedral coordination. This leaves only one model for the fit, that of two doublets with similar center shifts but different quadrupole splitting, which is consistent with a structure that shows two sites for Fe^{3+} with different degrees of distortion (Ishiguro *et al.* 1978).

The hyperfine parameters derived from the two fitted doublets with similar center-shifts and different quadrupole splitting are given in Table 4. The uncertainties are based on errors from the fit to the given model, as well as uncertainties in the model itself.

The center shifts fall well within the range expected for Fe^{3+} in octahedral coordination (McCammon 2000), and values of quadrupole splitting suggest that the site corresponding to doublet A is more distorted than that corresponding to doublet B (for Fe^{3+} there is only a lattice contribution, which is related to the distortion from cubic symmetry). This situation would seem to suggest that doublet A can be assigned to the Fe1 site, whereas doublet B can be assigned to the Fe2 site. The nearly equal area-ratios in the Mössbauer data are consistent with the structure refinement of Ishiguro *et al.* (1978), where Fe^{3+} is equally distributed between the two octahedral sites. On the whole, there is no evidence for Fe^{2+} in the Mössbauer data.

Secondary freudenbergite

Clustered together with ilmenite (Fig. 9), a second generation of freudenbergite was found in alkali syenite dike Kb 45. These late grains of freudenbergite around ilmenite grains formed owing to the breakdown

TABLE 2. REPRESENTATIVE RESULTS OF ELECTRON-MICROPROBE ANALYSES OF "LOW-TITANIUM" FREUDENBERGITE FROM VARIOUS DIKES, KATZENBUCKEL VOLCANO, SOUTHWESTERN GERMANY

sample	Kb18-15	Kb18-16	Kb34-03	Kb34-37	Kb40-33	Kb40-51	Kb41-14	Kb41-18	Kb45-15	Kb45-16	Kb50-18	Kb50-54
SiO_2 wt.%	0.00	0.00	0.00	0.00	0.00	0.00	0.01	0.00	0.01	0.00	0.01	0.01
TiO_2	69.68	67.13	70.46	68.98	66.65	70.47	67.91	70.05	64.59	68.12	71.35	69.72
ZrO_2	0.05	0.59	0.07	0.24	0.45	0.06	0.37	0.06	0.48	0.11	0.33	0.69
Nb_2O_5	1.98	4.84	1.84	3.06	5.97	1.62	2.78	1.24	5.47	1.90	0.65	0.50
Al_2O_3	0.00	0.00	0.00	0.00	0.00	0.00	0.00	0.00	0.00	0.00	0.00	0.00
Cr_2O_3	0.00	0.00	0.00	0.02	0.00	0.00	0.02	0.02	0.00	0.02	0.03	0.00
Fe_2O_3	19.84	19.09	18.84	19.15	17.06	17.92	18.48	18.89	20.30	20.92	18.61	19.70
MnO	0.19	0.18	0.08	0.09	0.44	0.26	0.16	0.09	0.09	0.06	0.05	0.05
MgO	0.67	0.90	0.70	0.79	1.36	1.02	0.78	0.74	0.74	0.44	1.00	0.58
CaO	0.03	0.05	0.07	0.07	0.04	0.01	0.06	0.07	0.06	0.05	0.00	0.01
Na_2O	8.55	8.19	8.50	8.61	8.36	8.79	8.64	8.66	8.30	8.90	8.82	8.93
K_2O	0.07	0.00	0.02	0.03	0.02	0.01	0.06	0.03	0.05	0.01	0.02	0.00
Total	101.06	100.98	100.58	101.04	100.35	100.15	99.28	99.85	100.08	100.51	100.86	100.18
Si *apfu*	0.000	0.000	0.000	0.000	0.000	0.000	0.001	0.000	0.001	0.000	0.001	0.001
Ti	6.032	5.851	6.107	5.981	5.843	6.128	5.993	6.115	5.713	5.951	6.153	6.083
Zr	0.003	0.033	0.004	0.013	0.026	0.004	0.021	0.003	0.027	0.006	0.018	0.039
Nb	0.103	0.254	0.096	0.159	0.315	0.085	0.148	0.065	0.291	0.100	0.034	0.026
Al	0.000	0.000	0.000	0.000	0.000	0.000	0.000	0.000	0.000	0.000	0.000	0.000
Cr	0.000	0.000	0.000	0.002	0.000	0.000	0.002	0.002	0.000	0.001	0.002	0.000
Fe^{3+}	1.718	1.665	1.634	1.661	1.497	1.559	1.632	1.650	1.797	1.829	1.606	1.720
Mn	0.019	0.018	0.008	0.009	0.043	0.026	0.016	0.009	0.009	0.006	0.005	0.005
Mg	0.115	0.155	0.120	0.136	0.236	0.176	0.137	0.127	0.129	0.076	0.171	0.100
Ca	0.004	0.006	0.009	0.009	0.005	0.001	0.007	0.009	0.007	0.006	0.000	0.001
Na	1.908	1.840	1.899	1.925	1.890	1.970	1.967	1.950	1.892	2.004	1.960	2.008
K	0.010	0.000	0.003	0.004	0.003	0.001	0.009	0.005	0.008	0.001	0.003	0.001
cations	9.911	9.823	9.880	9.899	9.858	9.948	9.934	9.935	9.874	9.980	9.954	9.983
oxygen atoms	16.000	16.000	16.000	16.000	16.000	16.000	16.000	16.000	16.000	16.000	16.000	16.000
A	1.922	1.847	1.911	1.938	1.899	1.972	1.983	1.964	1.907	2.011	1.963	2.010
B	1.852	1.838	1.762	1.808	1.776	1.761	1.787	1.788	1.935	1.913	1.785	1.825
T	6.137	6.138	6.207	6.154	6.183	6.216	6.162	6.184	6.031	6.057	6.205	6.147
B + *T*	7.989	7.976	7.969	7.962	7.959	7.976	7.950	7.972	7.966	7.970	7.990	7.973

Total Fe is given as Fe_2O_3. Compositions were calculated to 16 atoms of oxygen per formula unit (*apfu*).

of ilmenite in a late to post-magmatic environment. Chemically, this generation of freudenbergite is indistinguishable from primary freudenbergite.

Ilmenite in this dike formed early, whereas aegirine crystallized after amphibole, as is proven by ilmenite inclusions and overgrowths of aegirine on some of the amphibole grains. Primary freudenbergite crystallized later, either together with or shortly after the formation of aegirine, on the basis of inclusions or intergrowths of pyroxene in freudenbergite (*cf.* Fig. 3).

Moreover, in the same dike (Kb 45), freudenbergite occurs as thin lamellae within hematite. The plate-like freudenbergite has the appearance of exsolution lamellae (Fig. 10). In a cut parallel to (0001), the platelets are oriented in six different directions according to the symmetry of hematite along {0111}. Thus, the arrangement of freudenbergite lamellae in Figure 10 resembles Ramdohr's "blitz" texture, caused by exsolution "needles" of rutile in hematite (Ramdohr 1969, p. 964). Careful checking of the fine lamellae (Fig. 10) with a focused beam or semiquantitative SEM analyses invariably resulted in variable, but higher Na contents, in the range of 4.56–7.06 wt.% Na_2O. Electron-microprobe and SEM data show definitively that all the lamellae are composed of freudenbergite.

In a few cases, grains of hematite in sample Kb 45 were found to be protected in part by amphibole. A sector of such a shielded grain is shown in the high-resolution BSE image (Fig. 11). At the edges, one can see that freudenbergite works its way in from the exterior, predominantly along cracks or lenses of pre-existing exsolution-lamellae. The dark lamellae in Figure 11 are composed of freudenbergite, whereas the smaller, grey lamellae are not identified. They are too fine (≤0.2 μm)

TABLE 3. REPRESENTATIVE RESULTS OF ELECTRON-MICROPROBE ANALYSES OF "LOW-TITANIUM" AND "HIGH-TITANIUM" FREUDENBERGITE, KATZENBUCKEL VOLCANO, SOUTHWESTERN GERMANY

	Freudenbergite: "low-titanium" group						Freudenbergite: "high-titanium" group							
sample	Kb59a-16	Kb59a-17	Kb59a-30	Kb59-21	Kb59-28	mean	Kb59b-34	Kb59b-36	Kb59b-37	Kb59-06	Kb59-44	mean	Kb34-10	Kb40-60
SiO_2 wt.%	0.00	0.01	0.00	0.00	0.00	0.01	0.00	0.00	0.00	0.00	0.00	0.00	0.00	0.00
TiO_2	65.41	70.99	67.01	66.35	67.58	67.47	71.64	69.69	73.60	70.64	69.72	71.06	76.06	75.56
ZrO_2	0.25	0.01	0.16	0.20	0.13	0.15	0.18	0.23	0.20	0.51	0.39	0.30	0.04	0.00
Nb_2O_5	4.46	2.59	2.96	4.05	2.95	3.40	9.23	12.32	7.61	8.34	9.76	9.45	0.95	0.77
Al_2O_3	0.00	0.00	0.00	0.00	0.00		0.00	0.00	0.00	0.00	0.00		0.00	0.00
Cr_2O_3	0.05	0.00	0.01	0.00	0.00		0.00	0.00	0.03	0.01	0.04		0.01	0.00
Fe_2O_3	20.56	15.65	19.92	20.30	19.87	19.26	7.75	6.35	7.41	10.78	9.46	8.35	12.61	11.32
MnO	0.11	0.63	0.18	0.20	0.13	0.25	1.22	1.42	1.26	0.96	1.27	1.23	0.63	1.32
MgO	0.67	0.98	0.69	0.63	0.62	0.72	2.49	3.05	2.14	1.54	1.59	2.16	1.81	1.70
ZnO	0.10	0.19	0.04	0.06	0.03	0.08	0.37	0.36	0.42	0.74	0.89	0.55	n.d.	n.d.
CaO	0.05	0.06	0.06	0.07	0.05		0.03	0.06	0.05	0.02	0.01		0.03	0.05
Na_2O	8.10	8.32	8.39	8.28	8.27		7.06	6.77	6.94	6.76	6.70		8.55	8.82
K_2O	0.02	0.02	0.01	0.02	0.07		0.02	0.01	0.02	0.02	0.02		0.02	0.02
Total	99.79	99.45	99.43	100.15	99.69		100.00	100.26	99.67	100.30	99.84		100.72	99.56
Si *apfu*	0.000	0.001	0.000	0.000	0.000		0.001	0.000	0.000	0.000	0.000		0.000	0.000
Ti	5.787	6.205	5.920	5.839	5.949	5.940	6.200	6.042	6.360	6.134	6.097	6.167	6.475	6.514
Zr	0.015	0.001	0.009	0.011	0.007	0.009	0.010	0.013	0.011	0.029	0.022	0.017	0.002	0.000
Nb	0.237	0.136	0.157	0.214	0.156	0.180	0.480	0.642	0.395	0.435	0.513	0.493	0.049	0.040
Al	0.000	0.000	0.000	0.000	0.000		0.000	0.000	0.000	0.000	0.000		0.000	0.000
Cr	0.005	0.000	0.001	0.000	0.000		0.000	0.000	0.002	0.001	0.003		0.001	0.000
Fe^{3+}	1.820	1.369	1.761	1.787	1.750	1.697	0.671	0.551	0.641	0.936	0.827	0.725	1.075	0.977
Mn	0.011	0.062	0.018	0.020	0.013	0.025	0.119	0.138	0.122	0.094	0.125	0.120	0.060	0.128
Mg	0.117	0.170	0.120	0.110	0.107	0.125	0.426	0.524	0.367	0.265	0.276	0.371	0.305	0.291
Zn	0.008	0.016	0.004	0.005	0.003	0.007	0.031	0.030	0.036	0.063	0.076	0.047	n.d.	n.d.
Ca	0.006	0.007	0.008	0.008	0.006		0.004	0.008	0.006	0.002	0.001		0.004	0.006
Na	1.847	1.875	1.910	1.877	1.876		1.575	1.513	1.547	1.512	1.510		1.877	1.960
K	0.003	0.004	0.002	0.003	0.010		0.002	0.002	0.003	0.003	0.002		0.003	0.002
cations	9.856	9.845	9.910	9.875	9.877	9.872	9.521	9.463	9.489	9.473	9.453	9.480	9.851	9.918
oxygen atoms	16.000	16.000	16.000	16.000	16.000		16.000	16.000	16.000	16.000	16.000		16.000	16.000
A site	1.857	1.886	1.919	1.888	1.891	1.888	1.581	1.522	1.555	1.516	1.514	1.538	1.883	1.968
B site	1.961	1.617	1.903	1.922	1.873	1.855	1.247	1.244	1.168	1.358	1.308	1.265	1.441	1.396
T site	6.038	6.341	6.087	6.064	6.113	6.129	6.691	6.697	6.766	6.598	6.631	6.677	6.526	6.554
B + *T* sites	7.999	7.958	7.99	7.987	7.986	7.984	7.938	7.941	7.934	7.957	7.939	7.942	7.968	7.950

Total Fe is given as Fe_2O_3. Compositions were calculated on the basis of 16 atoms of oxygen.

for identification by analysis; in contrast to the freudenbergite lamellae (≤1.2 μm), Na is absent. Thus, all lamellae of freudenbergite in hematite are of secondary origin. They represent metasomatic replacements of primary exsolution-induced lamellae, likely of rutile or ilmenite. The latter segregations could be related to a process of incipient oxidation (Haggerty 1976, 1991).

Replacement of freudenbergite by lorenzenite

Lorenzenite was found in some of the alkali syenite rocks either as crystals ~100 μm long, intimately associated with aegirine, or as radiating bundles around grains of freudenbergite. In many cases, sheaf-like lorenzenite replaces freudenbergite (Fig. 12), which likely crystallized at a late stage of syenite formation.

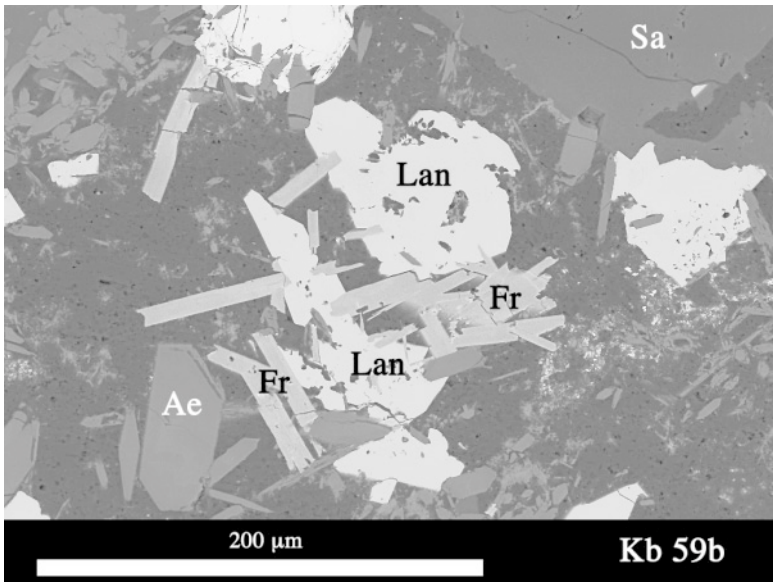

FIG. 7. Small tabular crystals of "high-titanium" freudenbergite (Fr) in coexistence with bright, anhedral grains of landauite (Lan). The BSE image is from alkali syenite dike Kb 59b. Sanidine (Sa) and coarser grains of aegirine (Ae) are present in the surroundings.

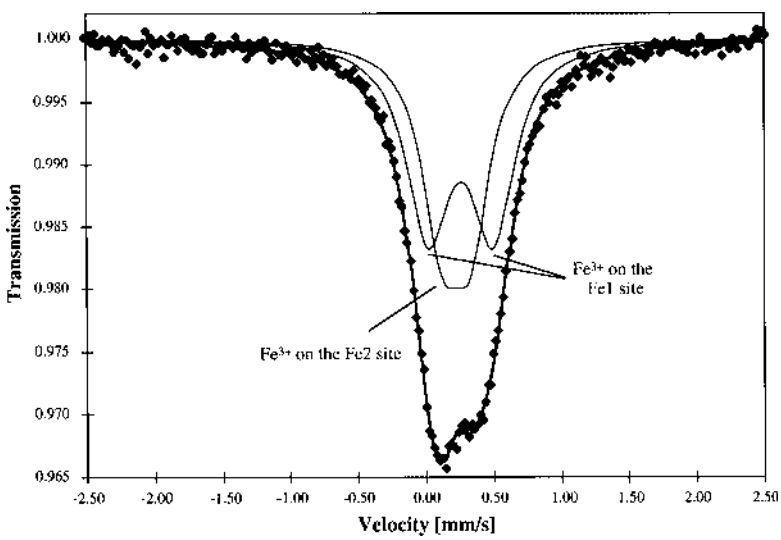

FIG. 8. Room-temperature Mössbauer spectrum of a "low-titanium" freudenbergite (Kb 34), fitted with two subspectra for Fe^{3+}, demonstrating that there is no Fe^{2+} present in these crystals.

Lorenzenite commonly occurs in alkaline rocks, notably in syenite pegmatites (Larsen *et al.* 1992). Although it is difficult to distinguish within masses of acicular or prismatic aegirine, its stronger birefringence and higher reflectivity enable identification in thin section. Results of four electron-microprobe analyses of lorenzenite are shown in Table 5. These late crystallizations at the expense of freudenbergite have higher Nb contents, in the range of 3.50 to 7.39 wt.% Nb_2O_5 and Fe contents between 1.26 to 1.94 wt.% Fe_2O_3. Higher amounts of these elements are indicative of a coupled substitution of Fe and Nb for Ti according to the schemes $Fe^{2+} + 2Nb^{5+} \rightleftharpoons 3Ti^{4+}$ and $Fe^{3+} + Nb^{5+} \rightleftharpoons 2Ti^{4+}$ (Larsen *et al.* 1992).

Pyrochlore, landauite and rare Na–Zr minerals as late-stage mineral phases

The majority of the samples of freudenbergite-bearing alkali syenite at Katzenbuckel contain pyrochlore as an accessory phase. In interstitial spaces among sanidine laths (Fig. 2), isometric grains of pyrochlore up to 200 μm in size occur as a late phase, in some cases intergrown with aegirine (Fig. 12). A few of the isometric grains show an atoll-like texture, with thin seams of newly grown pyrochlore at the rim (Fig. 12). In many cases, the pink grains of pyrochlore are optically and chemically zoned.

Representative results of analyses of pyrochlore (Table 6) show conspicuously high contents of Na (on average, 14.52 wt.% Na_2O), low contents of Ca (on average, 1.33 wt.% CaO) and very low atomic Ca:Na ratio. Using the nomenclature suggested by Hogarth (1989), this Na-rich mineral should be named sodian pyrochlore.

The structural formula of this mineral, calculated on the basis of two *B*-site cations (Nb + Ta + Ti + Zr), are close to the ideal formula $(Na,Ca)Nb_2O_6(F,OH)$. The pyrochlore at Katzenbuckel also shows moderate $LREE_2O_3$, SrO and TiO_2 contents and is enriched in Th (up to 4.82 wt.% ThO_2).

Coexisting with niobium-rich "high-titanium" freudenbergite, landauite occurs as a rare mineral in one of the alkali syenite samples (Kb 59). Landauite is a late mineral in the sequence of crystallization. Subhedral to anhedral grains partially enclose aegirine or parts of the freudenbergite prisms (Fig. 7). The mineral is opaque, with a slightly higher reflectivity than that of freudenbergite.

TABLE 4. HYPERFINE PARAMETERS OF MÖSSBAUER SPECTRA FROM LARGE CRYSTALS OF FREUDENBERGITE (KB 34) AT ROOM TEMPERATURE (293 K)

	Doublet A	Doublet B		Doublet A	Doublet B
CS [mm/s]	0.38(2)	0.34(2)	FWHM [mm/s]	0.38(2)	0.34(2)
QS [mm/s]	0.48(5)	0.21(5)	Area	0.55(13)	0.45(13)

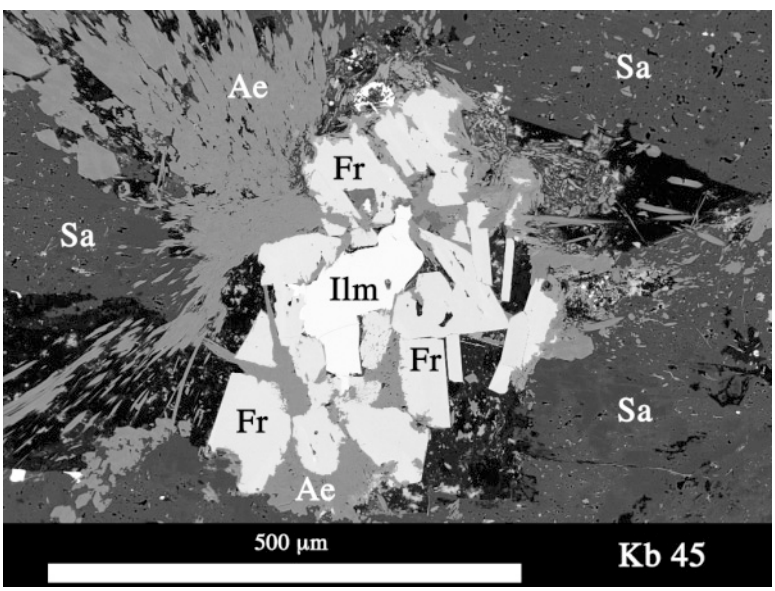

FIG. 9. BSE image of an unstable grain of ilmenite (Ilm) in sample Kb 45. The primary ilmenite is replaced by secondary freudenbergite (Fr). The oxide minerals are surrounded by sanidine (Sa) and aegirine (Ae).

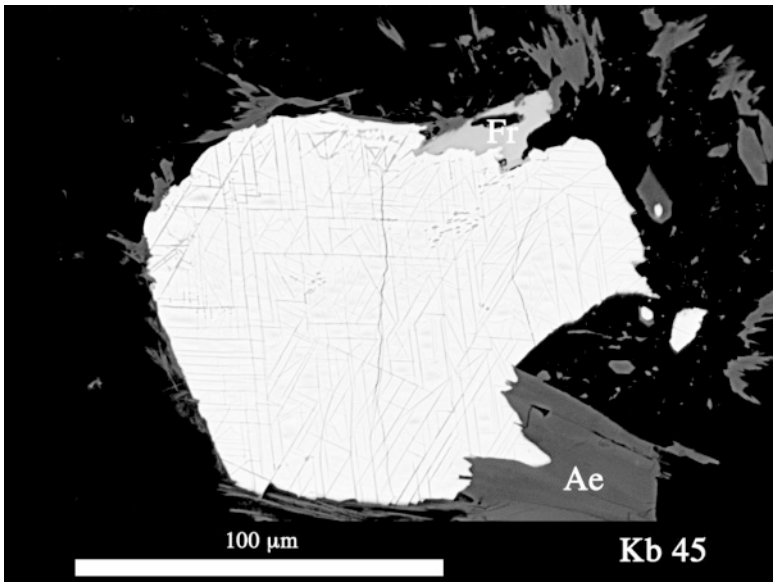

FIG. 10. Hematite with freudenbergite as "pseudo-exsolution" lamellae along rhombohedral planes. The lamellae are arranged in six different directions, visible in this section nearly perpendicular to [0001]. At the lower right of the BSE image, the grain of hematite is in contact with aegirine (Ae).

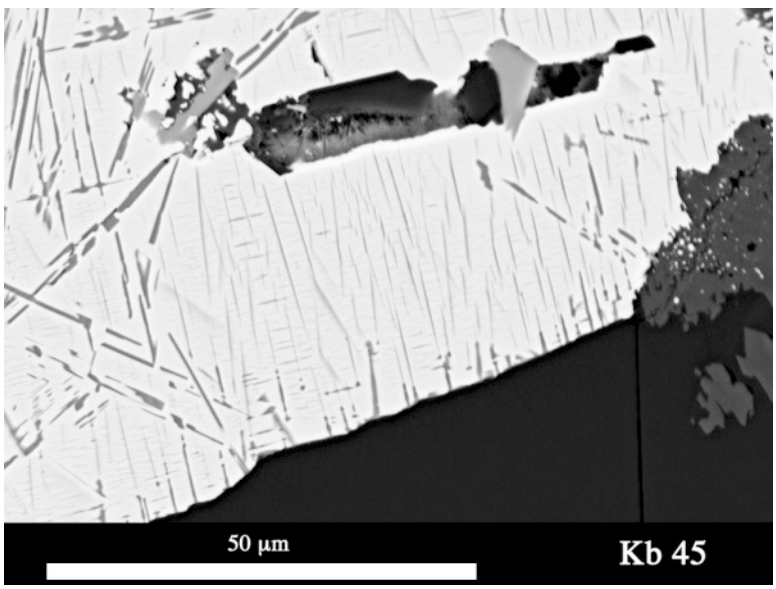

FIG. 11. High-resolution BSE image of the margin of a hematite grain. The small fine, grey lenses (central part of the image) are primary exsolution-lamellae (probably rutile or ilmenite). The dark lamellae are metasomatically formed freudenbergite "intruding" from the exterior.

Landauite belongs to the crichtonite group, with the general formula $AM_{21}O_{38}$ (Grey & Gatehouse 1978). Large-radius cations like Na or K occupy the *A* site, whereas smaller ions like Ti, Fe, Mn, Zn are found at the *M* sites. Representative results of electron-microprobe analyses are listed in Table 5. The sodium- and zinc-bearing compositions show higher niobium and manganese contents.

Late-stage crystallizations of rare Na–Zr minerals were found in interstitial spaces of some samples of alkali syenite (Fig. 2). Catapleiite and priderite have been confirmed on the basis of chemical data, but other tiny crystals remain unidentified.

Fe–Ti Oxides Coexisting with Freudenbergite

Among the suite of freudenbergite-bearing dikes, seven of the syenite samples contain oxides like pseudobrookite, ilmenite, hematite and magnetite (Table 1). The Fe–Ti oxides are sensitive indicators of redox conditions and prevailing temperatures (Haggerty & Baker 1967, Lindsley 1976) at the time of formation of the dikes.

Two of the dikes (Kb 50, Kb 59) containing pseudobrookite likely formed at temperatures above 600°C because pseudobrookite is known to break down at 585 ± 10°C to hematite and rutile, as was demonstrated experimentally by Haggerty & Lindsley (1970).

Five of the alkali syenite samples contain the opaque phases ilmenite and hematite in coexistence with freudenbergite. The compositions of Ilm_{ss} and Hem_{ss} pairs show variably broad gaps on the join $FeTiO_3$–Fe_2O_3. This is in accordance with experiments, where a distinct miscibility-gap exists at lower temperatures (Carmichael 1961, Lindsley 1973). If we interpret our data in terms of Lindsley's results, then the narrowest (Kb 50) and broadest (Kb 18) miscibility gap of the analyzed ilmenite–hematite pairs (Fig. 13, Table 7) lie within a temperature range of ~750–550°C.

Whole-Rock Geochemistry of the Freudenbergite-Bearing Syenites

Alkaline syenite dikes stem from felsic liquids as the latest products of differentiation of sanidine-bearing nephelinitic magma (Frenzel 1975). In our opinion, the evolved magma came from the highest levels of the magma chamber. Thus, comparison of the whole-rock compositions of the two rock types should give indications of the trend of magmatic evolution and, possibly, to the special circumstances leading to the formation of freudenbergite in alkali syenite at Katzenbuckel.

The composition of sanidine nephelinite and three samples of alkali syenite dikes is listed in Table 8. Ma-

TABLE 5. REPRESENTATIVE RESULTS OF ELECTRON-MICROPROBE ANALYSES OF LORENZENITE AND LANDAUITE, KATZENBUCKEL VOLCANO, SOUTHWESTERN GERMANY

	Lorenzenite				Landauite			
sample	Kb18-18	Kb18-30	Kb40-38	Kb40-68	Kb59-03	Kb59-08	Kb59-10	Kb59-14
SiO_2 wt.%	33.82	33.31	33.34	33.24	0.00	0.00	0.00	0.00
TiO_2	43.31	40.44	39.88	38.25	61.15	59.75	63.05	61.17
ZrO_2	0.36	0.48	0.27	0.38	1.51	1.63	2.07	1.99
Nb_2O_5	3.50	6.38	6.48	7.39	9.15	8.93	8.19	9.35
Al_2O_3	0.05	0.25	0.15	0.15	0.00	0.00	0.00	0.00
Cr_2O_3	0.00	0.02	0.02	0.00	0.00	0.01	0.00	0.00
Fe_2O_3	1.26	1.64	1.62	1.94	11.34	12.94	9.76	10.51
MnO	0.05	0.13	0.13	0.17	7.96	7.31	8.33	8.10
ZnO	n.d.	n.d.	n.d.	n.d.	4.44	4.78	3.44	3.77
MgO	0.09	0.15	0.16	0.15	1.37	1.25	1.53	1.48
CaO	0.09	0.10	0.05	0.05	0.08	0.07	0.11	0.15
Na_2O	17.30	17.05	17.33	17.33	1.54	1.48	1.50	1.44
K_2O	0.00	0.01	0.01	0.00	0.32	0.33	0.35	0.32
Total	99.83	99.96	99.44	99.04	98.84	98.45	98.31	98.27
Si *apfu*	1.956	1.941	1.954	1.963	0.000	0.000	0.000	0.000
Ti	1.883	1.772	1.757	1.699	13.400	13.191	13.778	13.449
Zr	0.010	0.014	0.008	0.011	0.214	0.233	0.293	0.283
Nb	0.092	0.168	0.172	0.197	1.205	1.184	1.076	1.236
Al	0.003	0.017	0.010	0.010	0.000	0.000	0.000	0.000
Cr	0.000	0.001	0.001	0.000	0.000	0.001	0.000	0.000
Fe^{3+}	0.055	0.072	0.072	0.086	2.485	2.858	2.133	2.312
Mn	0.002	0.006	0.006	0.008	1.963	1.817	2.050	2.005
Zn	n.d.	n.d.	n.d.	n.d.	0.954	1.036	0.738	0.813
Mg	0.008	0.013	0.014	0.013	0.595	0.547	0.662	0.647
Ca	0.006	0.006	0.003	0.003	0.025	0.022	0.034	0.047
Na	1.940	1.927	1.969	1.984	0.869	0.841	0.842	0.815
K	0.000	0.001	0.000	0.000	0.119	0.123	0.129	0.118
cations	5.954	5.939	5.967	5.975	21.830	21.852	21.735	21.725
oxygen atoms	9.000	9.000	9.000	9.000	38.000	38.000	38.000	38.000

Total Fe is given as Fe_2O_3. Compositions were calculated on the basis of 9 and 38 atoms of oxygen per formula unit (*apfu*), respectively.

TABLE 6. REPRESENTATIVE RESULTS OF ELECTRON-MICROPROBE ANALYSES OF PYROCHLORE, KATZENBUCKEL VOLCANO, SOUTHWESTERN GERMANY

sample	Kb18-03	Kb18-07		Kb18-03	Kb18-07
Na_2O wt.%	14.65	14.38	Na *apfu*	1.628	1.594
CaO	1.35	1.30	Ca	0.083	0.080
K_2O	0.16	0.12	K	0.012	0.009
SrO	1.76	1.81	Sr	0.059	0.060
FeO	0.35	0.21	Fe^{2+}	0.017	0.010
Al_2O_3	0.26	0.21	Al	0.018	0.014
La_2O_3	0.59	0.70	La	0.012	0.015
Ce_2O_3	3.72	4.01	Ce	0.078	0.084
Nd_2O_3	0.64	1.38	Nd	0.013	0.028
PbO	0.65	0.51	Pb	0.010	0.008
ThO_2	4.82	3.88	Th	0.063	0.051
Nb_2O_5	52.39	52.30			
Ta_2O_5	2.94	3.27	Total	1.993	1.953
TiO_2	13.61	13.59			
ZrO_2	0.36	0.45	Nb	1.357	1.352
			Ta	0.046	0.051
Total	98.25	98.12	Ti	0.586	0.584
			Zr	0.010	0.013
			Total	1.999	2.000

Compositions were calculated using the approach of Petruk & Owens (1975).

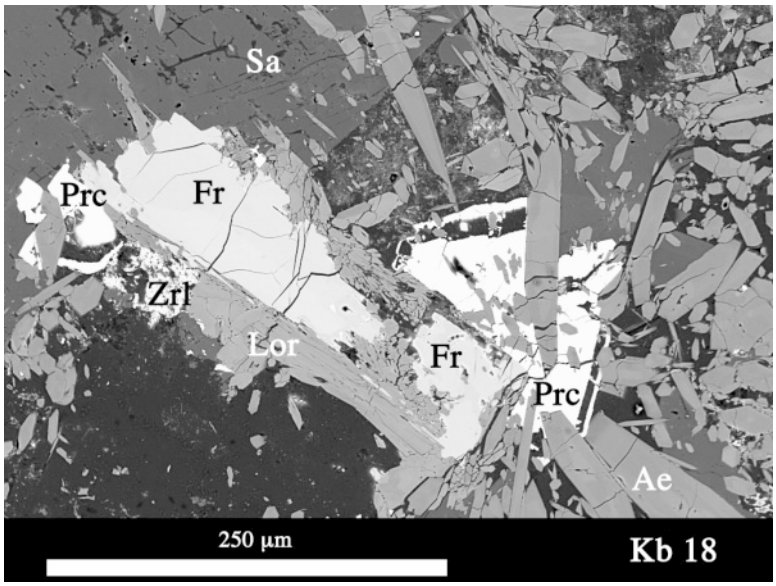

FIG. 12. BSE image of a freudenbergite crystal (Fr) that is partly replaced by needles or sheaves of lorenzenite (Lor). The bright, euhedral to subhedral grains are sodium-rich pyrochlore (Prc). Many crystals of prismatic aegirine (Ae), sanidine (Sa) and Na–Zr silicates (Zrl) are present in the surroundings.

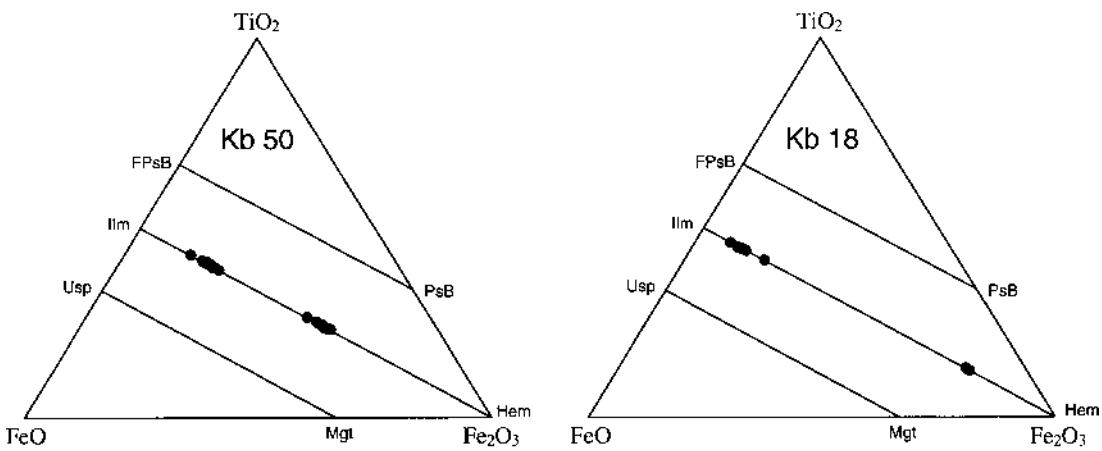

FIG. 13. Coexisting Fe–Ti oxides from two alkali syenite dikes (Kb 50, Kb 18) are plotted in the ternary diagram TiO_2–FeO–Fe_2O_3. The contents of Al_2O_3 and Cr_2O_3, MgO and MnO, ZrO_2 and Nb_2O_5 have been added to Fe_2O_3, FeO and TiO_2, respectively. The ilmenite–hematite pairs show large miscibility-gaps, which are indicative of crystallization temperatures in the range of 750–550°C (Lindsley 1973).

jor elements are in accordance with data published by Frenzel (1975); the unusually high contents of sodium, titanium and phosphorus in the nephelinites have been known for a long time.

By definition the alkali syenite dike rocks are peralkaline, with a molecular $(Na_2O + K_2O)/Al_2O_3$ ratio above 1.0 (Sørensen 1974, Le Maitre 1989). In comparison with the chemical composition of sanidine

nephelinite Kb 20, samples of alkali syenite show much higher concentrations of Nb and Zr, whereas CaO and MgO are distinctly lower (Table 8). In addition, the low contents of phosphorus and chlorine of the alkali syenites are especially remarkable.

Discussion

Within a suite of Katzenbuckel rocks, the mineral freudenbergite was found solely in some of the alkali syenite dikes. Evidently, high sodium and titanium contents accompanied by low concentrations of Ca have produced favorable conditions for the crystallization of this rare mineral.

Among the chemical ranges of freudenbergite, the predicted solid-solution series involving the continuous replacement of Fe^{3+} by Fe^{2+}, due to the coupled substitution $2Fe^{3+} \rightleftharpoons Fe^{2+}+Ti$, was not found. Mössbauer data for "low-titanium" freudenbergite indicate the absence of ferrous iron. Moreover, "high-titanium" freudenbergite, with its structural requirement for larger portions of divalent iron, shows the highest concentrations of Mg^{2+}, Mn^{2+} and Zn^{2+} of all the grains of freudenbergite analyzed. Possibly, elevated oxygen fugacities of the Katzenbuckel rocks limit the availability of ferrous iron within the alkali syenites. All volcanic rocks at Katzenbuckel have crystallized relatively close to the Earth's surface, and thus should contain Fe^{3+}.

The alkali syenite dikes show elemental concentrations typical for residual or evolved liquids. They were separated from the main sanidine nephelinite as less dense batches of volatile-rich liquid. Very likely, they accumulated in the roof zone of a magma chamber. They are the residuals after olivine and pyroxene fractionation, which may be inferred from their high SiO_2, similar Al_2O_3, but much lower MgO and CaO contents compared to the sanidine-bearing nephelinitic parental magma (Table 8).

A striking fact is that all chemically analyzed alkali syenites have low phosphorus and chlorine contents, whereas agpaitic rocks commonly are characterized by high to extreme contents of Na, Zr, Cl, F and P (Sørensen 1997). This fact correlates well with the findings of apatite and magnetite veins within Katzenbuckel rocks. Frenzel (1975) mentioned the presence of veins containing Cl-, F- and S-bearing apatite and fissures filled with magnetite. Some of the magnetite veinlets appear to have been re-opened and intruded later by an alkali syenitic melt, which would be indicative of a genetic relationship.

TABLE 7. REPRESENTATIVE RESULTS OF ELECTRON-MICROPROBE ANALYSES OF ILMENITE AND HEMATITE SOLID-SOLUTIONS, KATZENBUCKEL VOLCANO, SOUTHWESTERN GERMANY

	Kb50				Kb18			
sample	Ilm_{ss} Kb50-54	Ilm_{ss} Kb50-57	Hem_{ss} Kb50-56	Hem_{ss} Kb50-61	Ilm_{ss} Kb18-15	Ilm_{ss} Kb18-18	Hem_{ss} Kb18-20	Hem_{ss} Kb18-21
SiO_2 wt.%	0.00	0.00	0.00	0.02	0.00	0.01	0.01	0.00
TiO_2	42.59	42.15	27.19	25.08	44.97	44.70	13.34	13.04
ZrO_2	0.00	0.00	0.00	0.01	0.22	0.19	0.05	0.04
Nb_2O_5	0.42	0.50	0.17	0.15	0.77	0.59	0.00	0.04
Al_2O_3	0.00	0.00	0.00	0.00	0.00	0.00	0.00	0.00
Cr_2O_3	0.00	0.00	0.00	0.02	0.00	0.01	0.01	0.01
Fe_2O_3	19.29	20.17	48.10	52.41	10.43	11.93	76.19	75.52
FeO	28.41	28.19	20.09	18.47	34.16	33.57	6.18	7.37
MnO	5.80	5.65	2.76	2.07	1.43	1.82	2.09	2.31
ZnO	n.d.	n.d.	n.d.	n.d.	0.18	0.12	0.26	0.37
MgO	2.06	2.00	0.90	0.98	3.16	3.00	1.96	0.94
CaO	0.00	0.01	0.00	0.00	0.00	0.00	0.00	0.00
Na_2O	0.17	0.21	0.03	0.09	0.00	0.02	0.00	0.01
K_2O	0.00	0.00	0.01	0.00	0.00	0.00	0.00	0.01
Total	98.74	98.88	99.24	99.31	95.32	95.95	100.10	99.67
Si *apfu*	0.000	0.000	0.000	0.001	0.000	0.000	0.000	0.000
Ti	1.626	1.608	1.059	0.977	1.763	1.742	0.518	0.513
Zr	0.000	0.000	0.000	0.000	0.005	0.005	0.001	0.001
Nb	0.010	0.011	0.004	0.004	0.018	0.014	0.000	0.001
Al	0.000	0.000	0.000	0.000	0.000	0.000	0.000	0.000
Cr	0.000	0.000	0.000	0.001	0.000	0.000	0.000	0.000
Fe^{3+}	0.737	0.770	1.874	2.042	0.409	0.465	2.960	2.971
Fe^{2+}	1.206	1.196	0.870	0.800	1.489	1.455	0.267	0.322
Mn	0.249	0.243	0.121	0.091	0.063	0.080	0.092	0.102
Zn	n.d.	n.d.	n.d.	n.d.	0.007	0.005	0.010	0.014
Mg	0.156	0.151	0.069	0.076	0.245	0.232	0.151	0.073
Ca	0.000	0.001	0.000	0.000	0.000	0.000	0.000	0.000
Na	0.017	0.020	0.003	0.009	0.000	0.002	0.000	0.001
K	0.000	0.000	0.000	0.000	0.000	0.000	0.000	0.001
cations	4.000	4.000	4.000	4.000	4.000	4.000	4.000	4.000
oxygen atoms	6.000	6.000	6.000	6.000	6.000	6.000	6.000	6.000

Compositions were calculated to 4 cations and 6 atoms of oxygen.

TABLE 8. BULK COMPOSITION OF SANIDINE NEPHELINITE AND ALKALI SYENITE DIKES, KATZENBUCKEL VOLCANO, SOUTHWESTERN GERMANY

	Sanidine nephelinite	Alkali syenite				Sanidine nephelinite	Alkali syenite		
	Kb 20	Kb 18	Kb 34	Kb 41		Kb 20	Kb 18	Kb 34	Kb 41
SiO_2 wt %	38.07	53.69	56.76	53.55	Cl ppm	7254	50	115	62
TiO_2	3.74	2.75	2.22	2.22	F	1642	855	1007	746
Al_2O_3	12.28	13.65	10.69	15.90	Ba	1746	883	770	4206
Fe_2O_3 (1)	14.19	8.55	11.11	6.70	Ce	274	195	181	192
MnO	0.36	0.30	0.23	0.22	Co	6	< 5	< 5	9
MgO	4.80	1.68	1.83	1.81	Cr	< 5	< 5	< 5	< 5
CaO	7.57	1.32	1.36	1.55	Cs	17	< 5	11	7
Na_2O	7.77	7.53	6.33	6.46	La	482	113	156	192
K_2O	3.21	5.09	6.20	6.53	Nb	136	1683	319	462
P_2O_5	2.87	0.26	0.52	0.28	Ni	26	11	8	9
SO_3	0.70	0.01	0.04	0.01	Pb	13	70	29	54
					Rb	56	198	207	138
LOI (2)	0.97	2.68	1.11	2.56	Sr	2898	675	1249	2287
					Ta	< 5	151	22	13
Total	96.53	97.51	98.40	97.79	Th	15	282	29	40
					U	< 5	26	10	26
					V	198	84	78	99
Na_2O + K_2O	10.98	12.62	12.53	12.99	Y	45	98	34	42
					Zn	163	363	94	219
A. I.	1.32	1.31	1.60	1.11	Zr	918	6817	4014	2155

(1) All iron expressed as Fe_2O_3. (2) LOI: loss on ignition at 1000°C. A.I.: agpaitic index, the molar ratio $(Na_2O + K_2O)/Al_2O_3$ (Le Maitre 1989).

Segregations of apatite together with Fe–Ti oxides occur in a variety of geological settings. However, the origin of magnetite and apatite associations together with alkaline igneous rocks is unresolved, but the separation as immiscible liquid is one explanation among various hypotheses (Philpotts 1967, Mitsis & Economou-Eliopoulos 2001). Immiscibility of a Fe–P–O-enriched liquid from the ascending alkaline syenite magma would explain this association. On the other hand, it is unclear whether apatite contributes to the Cl depletion alone or if some Cl was lost during pre- or syn-eruptive degassing (Harms & Schmincke 2000).

We believe that important quantities of P, Ca, Cl and Fe were taken out from the felsic syenitic magma, and Na + Ti stayed behind, relatively enriched to form freudenbergite instead of Ca titanates. The unique occurrence of primary freudenbergite in alkali syenites was strongly influenced by shallow-level magmatic processes along with repeated and efficient fractionation. A late-stage prolonged differentiation, with fractionation and liquid immiscibility, probably led to felsic, Si-undersaturated, peralkaline rocks containing freudenbergite.

Summary and Conclusions

Peralkaline syenite dikes of the Katzenbuckel suite contain freudenbergite in coexistence with Fe–Ti oxides and some late-stage minerals such as lorenzenite, pyrochlore, landauite and rare Na–Zr silicates. Pseudobrookite and Ilm_{ss}–Hem_{ss} pairs allow temperature estimates in the range of 750–550°C. On the basis of their subvolcanic occurrence, the dikes were intruded into volcanic country-rocks at a low pressure, about 200–300 bars. If compared to silica-undersaturated massifs, the Katzenbuckel volcano can be classified as an alkaline complex with late-stage "pegmatitic" dikes or veins (Sørensen 1997).

Our systematic study of the freudenbergite crystals showed that:

1. Freudenbergite occurs exclusively in alkali syenite dikes.

2. It shows a great chemical variability, but evidence of a continuous substitution of Fe^{3+} by Fe^{2+} was not found. A Mössbauer spectrum of normal, coarser-grained freudenbergite demonstrates the existence of iron exclusively as Fe^{3+}.

3. Two types of freudenbergite were found in the dikes: a) Normal, "low-titanium" freudenbergite is equivalent to Frenzel's freudenbergite found in 1961. b) A "high-titanium" freudenbergite shows the highest contents of divalent ions (Mg + Mn + Zn), but the Fe^{2+}/Fe^{3+} value is still unknown. Small grain-sizes have prevented application of Mössbauer spectroscopy. Parts of the "high-titanium" freudenbergite have increased niobium concentrations and low sodium contents, which is indicative for cation deficiencies at the *A* site of the structure.

4. BSE-images reveal that some of the grains of freudenbergite are sector-zoned. Enrichments of (Nb + Zr) and Ti occur at different growth-sectors.

5. Metasomatically, freudenbergite may replace grains of ilmenite or exsolution lamellae found in hematite. In contrast, at late-stage conditions, lorenzenite replaces freudenbergite.

6. The unique occurrence of primary freudenbergite in Katzenbuckel rocks may be explained by extreme fractionation of an alkali-rich syenitic magma at very low pressures.

Acknowledgements

We thank R. Altherr, G. Brey and A. El Goresy for their critical comments and constructive advice. G. Frenzel, who collected some of the alkali syenite samples some years ago, is thanked for critical remarks. The authors are indebted to R. Borchardt (University Gießen) who performed two electron-microprobe analyses of pyrochlore. I. Glass and H.P. Meyer are gratefully acknowleged for their help with extensive BSE-imaging. We also thank M. Kaliwoda and N. Steppan for assistance with the collection of electron-microprobe data. We are also grateful to the critical reviewers, H. Sørensen, G. Ferraris and Associate Editor F. Vurro, whose constructive comments led to substantial improvement of the manuscript. We also thank R.F. Martin, who patiently corrected errors and infelicities of expression. Any remaining errors are solely our responsibility.

References

Bayer, G. & Hoffmann, W. (1965): Über Verbindungen vom Na_xTiO_2-Typ. *Z. Kristallogr.* **121**, 9-13.

_____ & _____ (1966): Complex alkali titanium oxides $A_x(B_yTi_{8-y})O_{16}$ of the α-MnO_2 structure type. *Am. Mineral.* **51**, 511-516.

Calvez, J.-Y. & Lippolt, H.J. (1980): Strontium isotope constraints to the Rhine Graben volcanism. *Neues Jahrb. Mineral., Abh.* **139**, 59-81.

Carmichael, C.M. (1961): The magnetic properties of ilmenite–hematite crystals. *R. Soc. London, Proc.* **A263**, 508-530.

Dowty, E. (1976): Crystal structure and crystal growth. II. Sector zoning in minerals. *Am. Mineral.* **61**, 460-469.

Flower, M.F.J. (1974): Phase relations of titan-acmite in the system Na_2O–Fe_2O_3–Al_2O_3–TiO_2–SiO_2 at 1000 bars total water pressure. *Am. Mineral.* **59**, 536-548.

Frenzel, G. (1955): Einführung in die Geologie und Petrographie des Katzenbuckels im Odenwald. *Aufschluss, Sh.* **2**, 48-56.

_____ (1960): Die neuerschlossene Schlotbreccie am Katzenbuckel im Odenwald und ihre Randgesteine. *Neues Jahrb. Mineral., Abh.* **94**, 1333-1358.

_____ (1961): Ein neues Mineral: Freudenbergit ($Na_2Fe_2Ti_7O_{18}$). *Neues Jahrb. Mineral., Monatsh.* 12-22.

_____ (1967): On petrochemistry and genesis of the volcanic rocks from the Katzenbuckel (Odenwald). *Abh. Geol. Land. Bad.-Württ.* **6**, 131-133.

_____ (1975): Die Nephelingesteinsparagenese des Katzenbuckels im Odenwald. *Aufschluss, Sb.* **27** (Odenwald), 213-228.

_____, OTTEMANN, J. & NUBER, B. (1971): Neue Untersuchungen an Freudenbergiten. *Neues Jahrb. Mineral., Monatsh.* 547-551.

FREUDENBERG, W. (1906) Geologie und Petrographie des Katzenbuckels im Odenwald. *Mitt. Bad. Geol. Landesanst.* **5**, 185-344.

GEHNES, P. & WIMMENAUER, W. (1975): Geochemical studies on igneous rocks of the Rhine Graben region (Germany). *Neues. Jahrb. Mineral., Monatsh.*, 49-56.

GREY, I.E. & GATEHOUSE, B.M. (1978): The crystal structure of landauite, $Na[MnZn_2(Ti,Fe)_6Ti_{12}]O_{38}$. *Can. Mineral.* **16**, 63-68.

HAGGERTY, S.E (1976): Opaque mineral oxides in terrestrial igneous rocks. *In* Oxide Minerals (D. Rumble III, ed.). *Rev. Mineral.* **3**, Hg 101-Hg 300.

_____ (1983): A freudenbergite-related mineral in granulites from a kimberlite in Liberia, West Africa. *Neues Jahrb. Mineral., Monatsh.*, 375-384.

_____ (1987): Metasomatic mineral titanates in upper mantle xenoliths. *In* Mantle Xenoliths (P.H. Nixon, ed.). John Wiley and Sons, New York, N.Y. (671-690).

_____ (1991): Oxide textures - a mini-atlas. *In* Oxide Minerals: Petrologic and Magnetic Significance (D.H. Lindsley, ed.). *Rev. Mineral.* **25**, 129-219.

_____ & BAKER, I. (1967): The alteration of olivine in basaltic and associated lavas. *Contrib. Mineral. Petrol.* **16**, 233-257.

_____ & LINDSLEY, D.H. (1970): Stability of the pseudobrookite (Fe_2TiO_5) – ferropseudobrookite ($FeTi_2O_5$) series. *Carnegie Inst. Wash., Year Book* **68**, 247-249.

HARMS, E. & SCHMINCKE, H.-U. (2000): Volatile composition of the phonolitic Laacher See magma (12,900 yr BP): implications for syn-eruptive degassing of S, F, Cl and H_2O. *Contrib. Mineral. Petrol.* **138**, 84-98.

HOGARTH, D.D. (1989): Pyrochlore, apatite and amphibole: distinctive minerals in carbonatites. *In* Carbonatites: Genesis and Evolution, (K. Bell, ed.). Unwin Hyman, London, U.K. (105-148).

ISHIGURO, T., TANAKA, K., MARUMO, F., ISMAIL, M.G.M.U., HIRANO, S. & SOMIYA, S. (1978): Freudenbergite. *Acta Crystallogr.* **B34**, 255-256.

JENSEN, B.B. (2000): Partitioning of elements in sector-zoned clinopyroxenes. *Mineral. Mag.* **64**, 725-728.

LARSEN, A.O., RAADE, G. & SÆBØ, P.C. (1992): Lorenzenite from the Bratthagen nepheline syenite pegmatites, Lagendalen, Oslo Region, Norway. *Norsk Geol. Tidsskr.* **72**, 381-384.

LARSEN, L.M. (1981): Sector zoned aegirine from the Ilímaussaq alkaline intrusion, South Greenland. *Contrib. Mineral. Petrol.* **76**, 285-291.

LE MAITRE, R.W. (1989): *A Classification of Igneous Rocks and Glossary of Terms*. Blackwell, Oxford, U.K.

LINDSLEY, D.H. (1973): Delimitation of the hematite–ilmenite miscibility gap. *Geol. Soc. Am., Bull.* **84**, 657-662.

_____ (1976): Experimental studies of oxide minerals. In Oxide Minerals (D. Rumble III, ed.). *Rev. Mineral.* **3**, L61-L88.

LIPPOLT, H.J., GENTNER, W. & WIMMENAUER, W. (1963): Altersbestimmungen nach der Kalium–Argon-Methode an tertiären Eruptivgesteinen Südwestdeutschlands. *Jahrb. Geol. Land. Bad.-Württ.* **6**, 507-538.

_____, HORN, P. & TODT, W. (1976): Kalium–Argon-Altersbestimmungen an tertiären Vulkaniten des Oberrheingraben-Gebietes. IV. Kalium–Argon-Alter von Mineralen und Einschlüssen der Basalt-Vorkommen Katzenbuckel und Roßberg. *Neues Jahrb. Mineral., Abh.* **127**, 242-260.

MCCAMMON, C.A. (1994): A Mössbauer milliprobe: practical considerations. *Hyperfine Interactions* **92**, 1235-1239.

_____ (2000): Insights into phase transformations from Mössbauer spectroscopy. *In* Transformation Processes in Minerals (S.A.T. Redfern & M.A. Carpenter, eds.). *Rev. Mineral.* **39**, 241-264.

_____, CHASKER, V. & RICHARDS, G.G. (1991): A technique for spatially resolved Mössbauer spectroscopy applied to quenched metallurgical slags. *Measure. Sci. Tech.* **2**, 657-662.

MCKIE, D. (1963): The unit-cell of freudenbergite. *Z. Kristallogr.* **119**, 157-160.

_____ & LONG, J.V.P. (1970): The unit-cell contents of freudenbergite. *Z. Kristallogr.* **132**, 157-160.

MITSIS, I. & ECONOMOU-ELIOPOULOS, M. (2001): Occurrence of apatite associated with magnetite in an ophiolite complex (Othrys), Greece. *Am. Mineral.* **86**, 1143-1150.

OKRUSCH, M., SCHUBERT, W. & STÄHLE, V. (2000): The Odenwald, Germany: Variscan metamorphic evolution and igneous events. *Eur. J. Mineral.* **12**, 45-89.

PATCHEN, A.D., TAYLOR, L.A. & POKHILENKO, N. (1997): Ferrous freudenbergite in ilmenite megacrysts: a unique paragenesis from the Dalnaya kimberlite, Yakutia. *Am. Mineral.* **82**, 991-1000.

PETRUK, W. & OWENS, D.R. (1975): Electron microprobe analyses for pyrochlores from Oka, Quebec. *Can. Mineral.* **13**, 282-285.

PHILPOTTS, A.R. (1967): Origin of certain iron–titanium oxide and apatite rocks. *Econ. Geol.* **62**, 303-315.

PRESTEL, D.J. (1992): *The Synthesis and Crystal Structures of Potassium and Cesium Hollandites and Sodium Freudenbergite*. Ph.D. thesis, Univ. of Illinois, Chicago, Illinois.

RAMDOHR, P. (1969): *The Ore Minerals and Their Intergrowths* (3rd ed.). Pergamon, Oxford, U.K.

ROSENBUSCH, H. (1869): *Der Nephelinit vom Katzenbuckel*. Ph.D. thesis (Inaug. Diss.), Univ. of Freiburg, Freiburg, Germany.

SØRENSEN, H. (1974): Alkali syenites, feldspathoidal syenites and related lavas. *In* The Alkaline Rocks. (H. Sørensen, ed.). John Wiley and Sons, London, U.K. (22-52).

_____ (1997): The agpaitic rocks - an overview. *Mineral. Mag.* **61**, 485-498.

VON LEONHARD, K.C. & GMELIN, L. (1822): *Nephelin in Dolerit am Katzenbuckel*. Mohr und Winter, Heidelberg, Germany.

WADSLEY, A.D. (1964): The possible identity of freudenbergite and Na_xTiO_2. *Z. Kristallogr.* **120**, 396-398.

WILSON, M. & DOWNES, H. (1991): Tertiary–Quaternary extension-related alkaline magmatism in western and central Europe. *J. Petrol.* **32**, 811-849.

WIMMENAUER, W. (1974): The alkaline province of central Europe and France. *In* The Alkaline Rocks (H. Sørensen, ed.). John Wiley and Sons, London, U.K. (238-271).

Received July 20, 2002, revised manuscript accepted November 8, 2002.